Solitary waves in the nonlinear Schrödinger equation with Hermite-Gaussian modulation of the local nonlinearity

Wei-Ping Zhong, Milivoj R. Belić, Boris A. Malomed, and TingWen Huang

Phys. Rev. E **84**, 046611 — Published 28 October 2011

DOI: 10.1103/PhysRevE.84.046611

Solitary waves in the nonlinear Schrödinger equation with Hermite-Gaussian modulation of the local nonlinearity

Wei-Ping Zhong[*1], Milivoj R. Belić[2,3], Boris A Malomed[4,5], and TingWen Huang[2]

[1] *Department of Electronic and Information Engineering, Shunde Polytechnic, Guangdong Province, Shunde 528300, China*

[2] *Texas A&M Univsersity at Qatar, P.O. Box 23874 Doha, Qatar*

[3]*Institute of Physics, University of Belgrade, P.O. Box 68 Belgrade, Serbia*

[4]*Department of Physical Electronics, School of Electrical Engineering, Faculty of Engineering, Tel Aviv University, Tel Aviv 69978, Israel*

[5]*ICFO-Institut de Ciencies Fotoniques, Mediterranean Technology Park, 08860 Castelldefels (Barcelona), Spain*

* Corresponding author: zhongwp6@126.com

Abstract: We demonstrate "hidden solvability" of the nonlinear Schrödinger (NLS) equation whose nonlinearity coefficient is spatially modulated by Hermite-Gaussian functions of different order and the external potential is appropriately chosen. By means of an explicit transformation, this equation is reduced to the stationary version of the classical NLS equation, which makes it possible to use the bright and dark solitons of the latter equation to generate solitary-wave solutions in our model. Special kinds of explicit solutions, such as oscillating solitary waves, are analyzed in detail. The stability of these solutions is verified by means of direct integration of the underlying NLS equation. In particular, our analytical results suggest a way of controlling dynamics of solitary waves by an appropriate spatial modulation of the nonlinearity strength in Bose-Einstein condensates, through the Feshbach resonance.

PACS numbers: 03.75.Lm, 42.65.Tg, 05.45.Yv

1. Introduction

The nonlinear Schrödinger (NLS) equation is a ubiquitous model describing wave dynamics in dispersive nonlinear media [1, 2]. The universality of the NLS equation and the great number of its applications have been stimulating the search for soliton solutions of generalized NLS models, in which the coefficients accounting for the diffraction/dispersion effects and the strength of the nonlinearity depend on the spatial and/or temporal variables. Classical results in the form of bright solitons were obtained for the one-dimensional (1D) NLS equation with constant coefficients by means of the inverse-scattering-transform (IST) technique [1]. This was later generalized to discrete models, such as the celebrated Ablowitz-Ladik equation [1], and some other [3], and for the NLS equation with random coefficients [4]. Applications of the NLS equation to fiber optics have stimulated further studies of integrable inhomogeneous models, leading to the concepts of self-similar and non-autonomous solitons [5].

A particularly important setting for solitons is described by the 1D NLS equation with the harmonic potential and cubic nonlinearity. In this case the equation is usually named the Gross-Pitaevskii (GP) equation [6] and the harmonic potential may be time-dependent [7]. This equation has drawn a great deal of attention, due to its direct applications to the description of Bose-Einstein condensates (BECs) [6], photonic waveguides [2], and other stationary and nonstationary media [8]. Other applications include the study of nonlinear tunneling of spatial and temporal optical solitons in various materials, with a potential use in ultrafast photonic technologies [9].

As early as 1976, Chen and Liu [10] have extended the concept of soliton to the case of accelerated motion of solitary waves in linearly inhomogeneous plasma. It was shown that the IST method can be generalized to the NLS equation with a linear external potential, by allowing time-varying eigenvalues, which makes it possible to predict solitons with time-varying velocities but constant amplitudes. Although the generalized NLS equation studied in Ref. [10] can be transformed back to the standard form of the equation, the use of the IST technique with the time-dependent spectral parameter makes it possible to extend the concept of integrability, especially to models in nonlinear optics, see Ref. [11] and references therein. On the other hand, Calogero and Degasperis [12] have introduced the general class of soliton solutions to the non-autonomous Korteweg–de Vries equation with varying nonlinearity and dispersion, which were constructed by means of a similar method. In a related context, the peculiarities of one- and multi-soliton dynamics in the discrete NLS equations were investigated in Ref. [13]. The ‘‘ideal’’ soliton-like interaction scenarios for non-autonomous solitons were studied in Refs. [14, 15] for the generalized NLS equations with varying dispersion, nonlinearity, and dissipation or gain.

Matter-wave solitons in BEC have attracted a great deal of interest, too [16, 17]. The possibility of using the Feshbach resonance to control the effective nonlinearity [18] has stimulated analyses of diverse nonlinear phenomena induced by manipulations of the scattering length, either in time [19] or in space [20] (see recent review [21]). In nonlinear optics, recent developments [22, 23] have led to the prediction of another new class of solitary waves, the so-called optical similaritons, which arise when the interplay of nonlinearity, dispersion, and gain in a fiber amplifier causes the shape of an input pulse to converge to a self-similar asymptotic form.

In this work, we go beyond previous studies, by considering the spatial modulation of the local nonlinearity coefficient in the form of Hermite-Gaussian functions. The usefulness of this approach stems from the fact that, because these functions represent the fundamental modes of the guided linear optical waves, the corresponding modulation profile can easily be induced by a laser beam illuminating the condensate and controlling the local strength of the optically-induced Feshbach resonance, see Ref. [21] and references therein. We demonstrate “hidden solvability" of this NLS equation, by utilizing the “resonance coupling technique," known in the BEC theory. The concept of "hidden integrability" refers to the procedure of transforming a new generalized equation into its classical integrable form, allowing one to generate exact soliton solutions of the new equation using the known solutions of the classical integrable equation. We report several types of explicit bright and dark solitary-wave solutions, including oscillating solitons, in the settings based on the experimentally feasible nonlinearity-modulation patterns.

The paper is organized as follows. In Sec. 2, the model describing the wave propagation in the cubic nonlinear medium is presented and the transformation reducing it to the stationary 1D NLS equation with constant coefficients is reported. The corresponding exact solitary-wave solutions, found by means of an appropriate product ansatz, are also presented in Sec. 2. In Sec. 3, we consider the dynamics of the fundamental and higher-order solitary waves in detail, including the verification of their stability by means of direct integration. The latter is necessary, as the above-mentioned transformation is not valid for the nonstationary version of the target NLS equation with constant coefficients, hence the stability of the exact solutions is not guaranteed. Sec. 4 presents our conclusions.

2. The model and solitary-wave solutions

The one-dimensional NLS/GP equation with an external potential and a modulated nonlinearity can be written in the following scaled form:

$$i\frac{\partial u}{\partial z}+\frac{1}{2}\frac{\partial^2 u}{\partial x^2}+\chi(x)|u|^2 u+\left[V(z,x)-\frac{1}{2}x^2\right]u=0\ , \qquad (1a)$$

where, in terms of nonlinear optics, $u(z,x)$ is the complex envelope of the electromagnetic field, z is the propagation distance, and x is the transverse coordinate. The x-dependent nonlinearity coefficient is taken in the special form,

$$\chi(x) = k e^{-x^2/2} H_n(x), \tag{1b}$$

where $H_n(x)$ are Hermite polynomials, and k is a normalization constant, to be specified below. Further, $-V(z,x)$ is the potential function depending on both the propagation distance and the transverse coordinate, which is determined by the choice of the nonlinear medium. The one-dimensional GP equation has the same form as Eq. (1a), but with the coordinate z replaced by time. It describes the evolution of the BEC wave function, and may also give rise to the solitary-wave solutions (see, e.g., Refs. [7, 17, 20-22, 24]). For $n=0$, Eq. (1) was considered in Ref. [22]. In the analysis of matter waves in BEC, where the local nonlinearity may be controlled by an optical beam via the Feshbach-resonance technique [21], the choice of the modulation function in the form of Eq. (1b) is natural, as this profile corresponds to an exact solution of the linear transmission equation with the parabolic confining potential; see also Eq. (3) below.

Using "the resonance coupling technique," which has been widely used in the studies of BEC models (see, e.g., Refs. [25, 26]), we look for particular solitary-wave solutions of Eq. (1), in the form $u = u_0(x,z)u_1(x,z)$. Substituting this ansatz into Eq. (1), and assuming that the first function satisfies the linear Schrödinger equation with the harmonic-oscillator potential,

$$i\frac{\partial u_0}{\partial z} + \frac{1}{2}\frac{\partial^2 u_0}{\partial x^2} - \frac{1}{2}x^2 u_0 = 0, \tag{2a}$$

we arrive at the following equation for $u_1(x,z)$:

$$i\frac{\partial u_1}{\partial z} + \frac{1}{2}\frac{\partial^2 u_1}{\partial x^2} + \frac{u_0^*}{|u_0|^2}\frac{\partial u_0}{\partial x}\frac{\partial u_1}{\partial x} + \chi|u_0|^2|u_1|^2 u_1 + V u_1 = 0. \tag{2b}$$

Commonly known solutions to Eq. (2a), subject to the normalization condition $\int_{-\infty}^{+\infty}|u_0|^2 dx = 1$, are [27]:

$$u_0 = k e^{-\frac{x^2}{2} - i\left(n+\frac{1}{2}\right)z} H_n(x), \tag{3}$$

where the normalization factor is $k = \sqrt{1/2^n n! \sqrt{\pi}}$, and $n = 0,1,\cdots$ is a non-negative integer. Accordingly, Eq. (2b) becomes

$$i\frac{\partial u_1}{\partial z} + \frac{1}{2}\frac{\partial^2 u_1}{\partial x^2} + h(x)\frac{\partial u_1}{\partial x} + g(x)|u_1|^2 u_1 + V u_1 = 0, \tag{4}$$

where $g(x) \equiv k^3 H_n^3(x) e^{-3x^2/2}$, and

$$h(x) \equiv \frac{u_0^*}{|u_0|^2}\frac{\partial u_0}{\partial x}. \tag{5}$$

In this work, we focus on the analysis of Eq. (4) with space-dependent coefficients $h(x)$ and $g(x)$. Our first goal is to transform Eq. (4) into the simple stationary NLS equation, cf. Ref. [28]:

$$EU + \frac{1}{2}\frac{d^2U}{d\theta^2} + GU^3 = 0, \tag{6}$$

where both $U \equiv U(\theta)$ and $\theta = \theta(z,x)$ are real functions, E denotes the eigenvalue (which corresponds to the chemical potential in BECs or to the propagation constant in optics), and $G = \pm 1$. We use below the classical soliton solutions of

Eq. (6), namely the bright soliton for $E<0$ and $G=1$,

$$U(\theta)=\sqrt{-2E}\operatorname{sech}\left(\sqrt{-2E}\theta\right), \tag{7a}$$

and the dark soliton for $E>0$ and $G=-1$,

$$U(\theta)=\sqrt{E}\tanh\left(\sqrt{E}\theta\right). \tag{7b}$$

To achieve the objective of reducing Eq. (4) to (6), we follow Refs. [22, 28] and look for the solutions of Eq. (4) in the form:

$$u_1(z,x)=\rho(z,x)U[\theta(z,x)]e^{i\varphi(z,x)}, \tag{8}$$

where ρ and φ are real functions. Substituting Eq. (8) into Eq. (4) and making use of Eq. (6), we arrive at the following set of coupled equations:

$$\left(\rho^2\right)_z+\left(\rho^2\varphi_x\right)_x+h\rho^2\varphi_x=0, \tag{9a}$$

$$\theta_z+\theta_x\varphi_x=0, \tag{9b}$$

$$\left(\rho^2\theta_x\right)_x+h\rho^2\theta_x=0, \tag{9c}$$

$$g\rho^2-G\theta_x^2=0, \tag{9d}$$

$$V(z,x)=\varphi_z-\frac{1}{2}\frac{\rho_{xx}}{\rho}+E\theta_x^2+\frac{1}{2}\varphi_x^2-h\frac{\rho_x}{\rho}, \tag{9e}$$

where the subscripts stand for the partial derivatives.

With regard to the definition given by Eq. (5), Eq. (9c) can be integrated, to yield

$$\rho^2=\frac{\lambda(z)}{|u_0|\theta_x}, \tag{10}$$

where $\lambda(z)$ is an arbitrary function of z. Next, from Eqs. (9d) and (10) one obtains $\theta_x=\sqrt[3]{\lambda/G}k^{2/3}H_n^{2/3}(x)e^{-x^2/3}$, hence

$$\theta(z,x)=\sqrt[3]{\frac{\lambda}{G}}k^{2/3}\int H_n^{2/3}(x)e^{-\frac{x^2}{3}}dx+\beta(z), \tag{11}$$

where $\beta(z)$ is another arbitrary function of z. Substituting ρ^2 from Eq. (10) into Eq. (9a) and using Eq. (9b), we obtain

$$\frac{\theta_{zx}\theta_x-\theta_z\theta_{xx}}{\theta_x^2}=\frac{\lambda_z}{2\lambda}. \tag{12}$$

Further, it follows from Eq. (9b) that

$$\varphi_{xx}(z,x)=-\frac{\theta_{zx}\theta_x-\theta_z\theta_{xx}}{\theta_x^2}. \tag{13}$$

Comparing Eqs. (12) and (13), we see that $\varphi(z,x)=-\frac{\lambda_z}{4\lambda}x^2+\delta(z)x+\varepsilon(z)$; here $\delta(z)$, and $\varepsilon(z)$ are additional arbitrary functions of z. Now, potential $V(z,x)$ can be expressed in terms of functions $\lambda(z)$, $\delta(z)$, $\varepsilon(z)$ and $\theta(z,x)$, using Eq. (9e):

$$V(z,x)=-\frac{\lambda\lambda_{zz}-\lambda_z^2}{4\lambda^2}x^2+\delta_z x+\varepsilon_z-\frac{1}{2}\frac{\rho_{xx}}{\rho}+E\theta_x^2+\frac{1}{2}\left(\frac{\theta_z}{\theta_x}+\delta\right)^2-h\frac{\rho_x}{\rho}, \tag{14}$$

where $\frac{\rho_x}{\rho}=-\frac{(|u_0|)_x\theta_x+|u_0|\theta_{xx}}{2|u_0|\theta_x}$ and $\frac{\rho_{xx}}{\rho}=\frac{3}{4}\cdot\frac{(|u_0|_x)^2\theta_x^2+|u_0|^2\theta_{xx}^2}{|u_0|^2\theta_x^2}-\frac{|u_0|_{xx}\theta_x-|u_0|_x\theta_{xx}+|u_0|\theta_{xxx}}{2|u_0|\theta_x}$.

Collecting the above results, we get the following particular solutions of Eq. (4):

$$u_1(z,x)=\left(\frac{|G|\lambda^2}{k^5|H_n(x)|^5}\right)^{1/6}e^{\frac{5}{12}x^2}U[\theta(z,x)]e^{i\left[-\frac{\lambda_z}{4\lambda}x^2+\delta(z)x+\varepsilon(z)\right]}, \tag{15}$$

from which the final form of the solutions for the solitary wave is obtained:

$$u(z,x)=u_0(z,x)u_1(z,x)=\sqrt[6]{\lambda^2k|GH_n(x)|}e^{-\frac{1}{12}x^2}U[\theta(z,x)]e^{i\left[-\frac{\lambda_z}{4\lambda}x^2+\delta(z)x+\varepsilon(z)-\left(n+\frac{1}{2}\right)z\right]}. \tag{16}$$

It follows from Eq. (16) that $u(z,x)\to 0$ when $|x|\to\infty$, if both the bright- and dark-soliton wave forms, (7a) and (7b), are substituted; hence this solution is always localized. In the next section, we exploit this fact to construct solitary-wave solutions exhibiting noteworthy behavior.

3. Examples of the solitary waves

The solutions presented below are obtained for the negative eigenvalues [$E<0$, which correspond to the bright solitons (7a)] and for the positive ones [$E>0$, which give rise to dark waves (7b)]. Recall that the arbitrary functions *β(z)* and *λ(z)* are important in our solution procedure, as they modulate the amplitude, the phase, and the independent variable *θ(z,x)* of the general solution in Eq. (16). Considering different choices of the functions $\lambda(z)$ and $\beta(z)$ brings widely different solutions; we single out two characteristic examples:

$$\lambda(z)=\lambda_0,\ \beta(z)=a\cos(\omega_0 z), \tag{17}$$

where $\lambda_0\neq 0$ is a constant, $a\in(0,1)$, and $\omega_0\neq 0$ (cf. Ref. [29]); and

$$\beta(z)=\beta_0,\ \lambda(z)=1+A\cos(\Omega_0 z), \tag{18}$$

where β_0 is a constant, $A\in(0,1)$, and $\Omega_0\neq 0$.

The former case deserves detailed consideration, as the corresponding solution (16) seems interesting. In Fig. 1, we plot examples of bright solitary-wave solutions, generated by the bright seed wave form (7a), which display a typical periodic behavior. The respective potential $V(z,x)$ is shown in the right column of the same figure. Thus, we can produce the bright solitary wave by adjusting the coefficients a and ω_0, which suggests a possibility to control the amplitude of the solitary wave oscillations and the curvature of its trajectory. Of course, it is possible to use the parameters in different ways to control the evolution of solitary waves. We conclude that the frequency of oscillations of the bright solitary wave increases with the increase in ω_0, and the amplitude of the peak's oscillation increases as the modulation amplitude a increases in Eq. (17).

The nonlinearity coefficient $\chi(x)$, given by Eq. (1b), is drawn in Fig. 1(c) for two values of n. As seen, there exists one maximum and no zeros for the Gaussian distribution $(n=0)$, while there are two extrema and one zero for $n=1$. In general, there exist $n+1$ extrema and n zeros along the x direction.

Fig.1

FIG. 1 (color online) Dynamics of the solitary wave (16) generated by the bright seed (7a), with $E=-1/2$, $G=1$, $\lambda_0=1$, $a=0.5$, $\varepsilon=0$, and $\omega_0=2$. The intensity of the solitary wave (left) and the shape of the external potential (right) are displayed, for $n=0$ and $n=1$, in panels (a) and (b). (c) Nonlinearity coefficient $\chi(x)$ vs x for $n=0$ and 1, see Eq. (1b).

Now, we proceed to the solutions generated by the dark seed solitary wave (7b). In Fig. 2, we display the corresponding spatial distribution of the soliton's intensity for different values of n, according to Eqs. (16), (7b), and (17). The plots in Fig. 2(a) correspond to $n=0$, $\omega_0=2$, $a=0.2$, $\lambda_0=1$, $E=1$ and $G=-1$, while Fig. 2(b) corresponds to $n=2$ and $\omega_0=4$; other parameters are the same as in Fig. 2(a).

Comparing Figs. 1 and 2, a difference in the shapes of solitons of order n, generated by the bright and dark seeds, becomes evident: while the solutions of both types are effectively localized, they feature $n+1$ and $n+2$ lobes, respectively. The extra lobe in the latter case appears due to the presence of the node in the center of the dark-soliton seed.

Fig.2

FIG. 2 (color online) Plots of the breathing solitary waves (16) generated by the dark seed (7b) (the corresponding parameters are given in the text). The setup here and in Figs. 3 and 4 below is the same as in Fig. 1(a)-(b).

Next, we proceed to the modulation functions taken as per Eq. (18). Specific higher-order solitary-wave solutions, given by Eq. (16), can be constructed in this case, if the modulation amplitude in Eq. (18) is small, $A \ll 1$. In Fig. 3, we show the fourth-order ($n=4$) bright solitary wave for the parameter set $\beta_0=0$, $A=0.1$, $\Omega_0=5$, $E=-1/2$, and $G=1$. It is seen that the intensity displays five lobes. The amplitude of the oscillations of each lobe increases with the distance of the lobes from $x=0$. Notice that the soliton's intensity is smallest at the center ($x=0$), but it does not approach zero. It is observed that the local intensity displays $n+1$ maxima for such a type of bright solitary waves.

Fig.3

FIG. 3 (color online) Fourth-order bright solitary wave. The corresponding parameters are given in the text.

As we have already demonstrated, Eq. (16) also produces higher-order solitary-wave solutions from the dark seed given by Eq. (7b). Here we consider a typical example for the following set of parameters: $\beta_0=0$, $A=0.1$, $\Omega_0=5$, $E=1$ and $G=-1$, using the modulation according to Eq. (18). The fourth-order soliton generated by the dark wave seed is plotted in Fig. 4. The comparison of Figs. 3 and 4 demonstrates the difference in the shape of the intensities of bright and dark solitary waves. Although the soliton obtained from the dark seed also displays five lobes, the intensity of the lobes increases with the distance from the center ($x=0$). Note that the soliton's intensity vanishes at $x=0$, as it should.

We also see that, for the solitary waves generated by the dark seed, the properly chosen external potential is very different from its counterpart supporting the solitary wave from the bright seed, cf. Fig. 3. Namely, while the parabola-shaped potential attains its maximum at the center ($x=0$) for the solitons of the latter type, the potential associated with the dark seed displays a double-well shape.

Fig.4

FIG. 4 (color online) Fourth-order ($n=4$) solitary wave (16) generated by the dark seed-wave form (7b). The corresponding parameters are given in the text.

One should note that the transformation leading to the NLS equation (6) is relevant only for the stationary form of this equation, hence it does not imply anything about the stability of the so-generated soliton solutions. To confirm the validity of solution (16) and test the stability of solitons, we have compared the analytical solution with the results of numerical simulations of the underlying equation (1). Figure 5 shows the comparison of the exact solution given by Eq. (16) with the results of simulations, produced by means of the split-step beam-propagation method [31]. The initial conditions were taken from the analytical solution (16) at $z=0$. It is seen that the analytical solution is consistent with the numerical results, and the solitary waves are stable indeed.

Fig.5

Fig. 5. (Color online) Comparison of the analytical solution with the numerical simulations at different propagation distances. The black solid line is the analytical solution given by Eq, (16) and the dashed red line is the result of the simulation of Eq. (1). (a) The setup is the same as in Fig.1 (a), the propagation distance being $z=10,20,30,60$ from left to right. (b) The same as in (a), except for $n=3$; the propagation distance is $z=10,30,60$ from bottom to top.

It is relevant to mention that the dynamical stability of the predicted analytical solutions also suggests the *structural stability* of the solutions reported above. Indeed, the solutions corresponding to the nonlinearity function and the potential slightly different from those selected for generating the exact solutions [see Eq. (5) and (14)] are expected to converge to the shapes only slightly different from those corresponding to the particular exact solutions.

4、Conclusions

In this work, we have extended previous works aimed at finding physically relevant special examples of the one-dimensional NLS/GP equation with the "hidden integrability", which means that it may be explicitly transformed into the classical integrable form, allowing one to find a broad class of exact soliton solutions. Here, we have demonstrated that this is possible for the NLS/GP equation with the spatial nonlinearity-modulation pattern based on the classical Hermite-Gaussian functions, which, in terms of BEC, can be realized by an external laser illumination via the Feshbach resonance, combined with the properly chosen harmonic trapping potential. The stability of the so-found special solutions was verified by means of direct integration of the full underlying equation.

The method elaborated here may be extended to the study of (2+1)-dimensional and (3+1)-dimensional models (cf. Ref. [28]), which are important for both matter waves and nonlinear optics [30].

This work was supported by the Natural Science Foundation of Guangdong Province, China, under Grant No. 1015283001000000. The work at the Texas A&M University at Qatar is supported by the NPRP 25-6-7-2 and NPRP 09-462-1-074 projects of the Qatar National Research Foundation.

References

[1] V. E. Zakharov and A. B. Shabat, Zh. Eksp. Teor. Fiz. **61**, 118 (1971) [English translation: Sov. Phys. JETP **34**, 62 (1972)]; V. E. Zakharov, S. V. Manakov, S. P. Novikov and L. P. Pitaevskii, *Solitons: The Inverse Scattering Transform Method* (Nauka, Moscow, 1980) [English translation: 1984 (Consultants Bureau, New York, 1984)]; M. J. Ablowitz and H. Segur, *Solitons and Inverse Scattering Transform* (SIAM, Philadelphia: 1981).

[2] C. Sulem and P. L. Sulem, *The Nonlinear Schrödinger Equation: Self-focusing and Wave Collapse* (Springer-Verlag, New York, 1999); Y. S. Kivshar and G. P. Agrawal, *Optical Solitons: From Fibers to Photonic Crystals* (Academic, New York, 2003).

[3] R. Scharf and A. R. Bishop, Phys. Rev. A **43**, 6535 (1991); V. V. Konotop, O. A. Chubykalo, and L. Vázquez, Phys. Rev. E **48**, 563 (1993).

[4] I. M. Besieris, in *Nonlinear Electromagnetics*, edited by P. L. E. Uslenghi (Academic Press, New York, 1980).

[5] S. A. Ponomarenko and G. P. Agrawal, Phys. Rev. Lett. **97**, 013901(2006).

[6] F. Dalfovo, S. Giorgini, L. P. Pitaevskii, and S. Stringari, Rev. Mod. Phys. **71**, 463 (1999); L. P. Pitaevski and S. Stringari, *Bose-Einstein Condensation* (Oxford University Press, Oxford, 2003).

[7] B. B. Baizakov, G. Filatrella, B. A. Malomed, and M. Salerno, Phys. Rev. E **71**, 036619 (2005).

[8] B. A. Malomed, *Soliton Manegement in Periodic Systems* (Springer, New York, 2006).

[9] D. Anderson, M. Lisak, B. Malomed, and M. Quiroga-Teixeiro, J. Opt. Soc. Am. B **11**, 2380 (1994); V. N. Serkin, V. M. Chapela, J. Percino, and T. L. Belyaeva, Opt. Commun. **192**, 237 (2001).

[10] H. H. Chen and C. S. Liu, Phys. Rev. Lett. **37**, 693 (1976); Phys. Fluids **21**, 377 (1978).

[11] S. P. Burtsev and I. R. Gabitov, Phys. Rev. A 49, 2065 (1994).

[12] F. Calogero and A. Degasperis, Lett. Nuovo Cimento **16**, 425 (1976); **16**, 434 (1976).

[13] V. V. Konotop, Phys. Rev. E **47**, 1423 (1993); V. V. Konotop, O. A. Chubykalo, and L. Vazquez, *ibid*. **48**,563 (1993).

[14] V. N. Serkin and A. Hasegawa, and T. L. Belyaeva, Phys. Rev. Lett. **98**, 074102 (2007); V. N. Serkin, A. Hasegawa, and T. L. Belyaeva, Phys. Rev. A **81**, 023610 (2010).

[15] V. N. Serkin, A. Hasegawa, and T. L. Belyaeva, Phys. Rev. Lett. **92**, 199401 (2004).

[16] K. E. Strecker, G. B. Partridge, A. G. Truscott, and R. G. Hulet, Nature (London) 417, 150 (2002); L. Khaykovich, F. Schreck, G. Ferrari, T. Bourdel, J. Cubizolles, L. D. Carr, Y. Castin, and C. Salomon, Science 296, 1290 (2002).

[17] *Emergent Nonlinear Phenomena in Bose-Einstein Condensates: Theory and Experiment*, edited by P. G. Kevrekidis, D. J. Frantzeskakis, and R. Carretero-Gonzalez (Springer, New York, 2008).

[18] S. Inouye, M. R. Andrews, J. Stenger, H.-J. Miesner, D. M. Stamper-Kurn, and W. Ketterle, Nature (London) **392**, 151 (1998); M. Theis, G. Thalhammer, K. Winkler, M. Hellwig, G. Ruff, R. Grimm, and J. Hecker Denschlag, Phys. Rev. Lett. **93**, 123001 (2004).

[19] P. G. Kevrekidis, G. Theocharis, D. J. Frantzeskakis and B. A. Malomed, Phys. Rev. Lett. **90** 230401 (2003); F. Kh. Abdullaev, A. M. Kamchatnov, V. V. Konotopp, and V. A. Brazhnyi, Phys. Rev. Lett. **90**, 230402 (2003); H. Saito and M. Ueda, Phys. Rev.

Lett. **90**, 040403 (2003); F. Kh. Abdullaev, J. G. Caputo, R. A. Kraenkel, and B. A. Malomed, Phys. Rev. A **67**, 013605 (2003); V. V. Konotop and P. Pacciani, Phys. Rev. Lett. **94**, 240405 (2005); A. Itin, T. Morishita, and S. Watanabe, Phys. Rev. A **74**, 033613 (2006).

[20] M. I. Rodas-Verde, H. Michinel, and V. M. Perez-Garcıa, Phys. Rev. Lett. **95**, 153903 (2005); H. Sakaguchi and B. A. Malomed, Phys. Rev. E **72**, 046610 (2005); G. Theocharis, P. Schmelcher, P. G. Kevrekidis, and D. J. Frantzeskakis, Phys. Rev. A **72**, 033614 (2005); V. M. Pérez-Garcia, P. J. Torres, and V. V. Konotop, Physica D 221, 31 (2006).

[21] Y. V. Kartashov, B. A. Malomed, and L. Torner, Rev. Mod. Phys. **83**, 247 (2011).

[22] J. Belmonte-Beitia, V. M. Perez-Garcia, and V. Vekslerchik, Phys. Rev. Lett. **98**, 064102 (2007); *ibid*. **100**,164102 (2008); J. Belmonte-Beitia and J. Cuevas, J. Phys. A: Math. Theor. **42**, 165201 (2009)

[23] S. A. Ponomarenko and G. P. Agrawal, Phys. Rev. Lett. **97**, 013901 (2006); J. M. Dudley, C. Finot, D. J. Richardson and G. Millot, Nature Phys. **3**, 597(2007).

[24] W. P. Zhong and M. Belić, Phys. Rev. E **81**, 056604 (2010); T. G. Akin, S. Kennedy, B. Dribus, J. Marzuola, L. Johnson, J. Alexander, and E. R. I. Abraham, preprint arXiv:1107.0016

[25] S. Jochim, M. Bartenstein, A. Altmeyer,G. Hendl, S. Riedl, C. Chin, J. Hecker Denschlag and R. Grimm. Science **302,** 2101 (2003).

[26] M. Greiner, C. A. Regal, and D. S. Jin, Nature **426,** 537 (2003).

[27] B. Yang, W. P. Zhong, and M. R. Belić, Commun.Theor. Phys. **53**, 937 (2010).

[28] V. M. Pérez-García, P. J. Torres, and V. V. Konotop, Physica D **221**, 31 (2006); A. T. Avelar, D. Bazeia, and W. B. Cardoso, Phys. Rev. E 79, 025602(R) (2009).

[29] A. I. Strinic, M. Petrovic, D. V. Timotijevic, N. B. Aleksic, and M. R. Belic, Opt. Express **17**, 11698 (2009).

[30] B. A. Malomed, D. Mihalache, F. Wise, and L. Torner, J. Opt. B 7, R53 (2005).

[31] M. Belic, N. Petrovic, W.P. Zhong, R.H. Xie and G. Chen, Phys. Rev. Lett. 101, 123904 (2008).

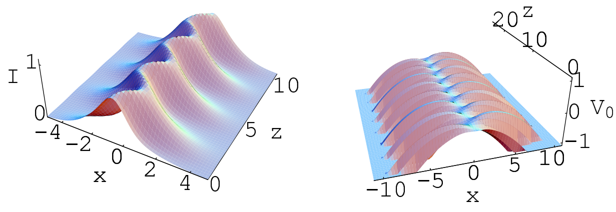

(a) n = 0

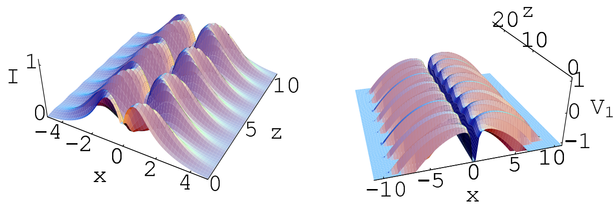

(b) n = 1

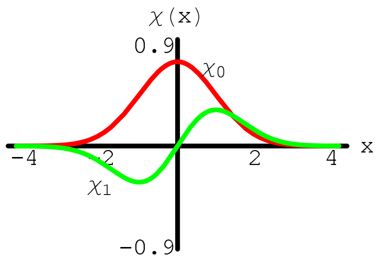

(c)

Figure 1 AF10902E 16SEP2011

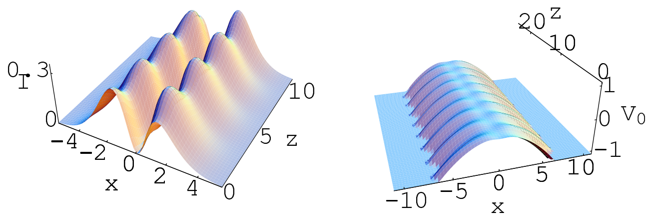

(a) n = 0

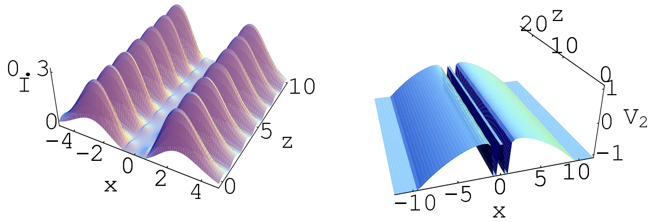

(b) n = 2

Figure 2 AF10902E 16SEP2011

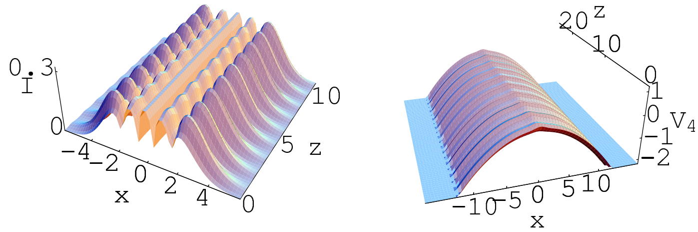

Figure 3 AF10902E 16SEP2011

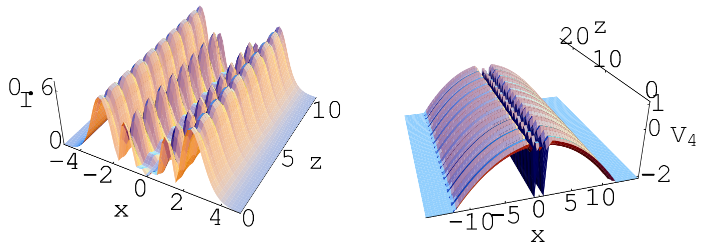

Figure 4 AF10902E 16SEP2011

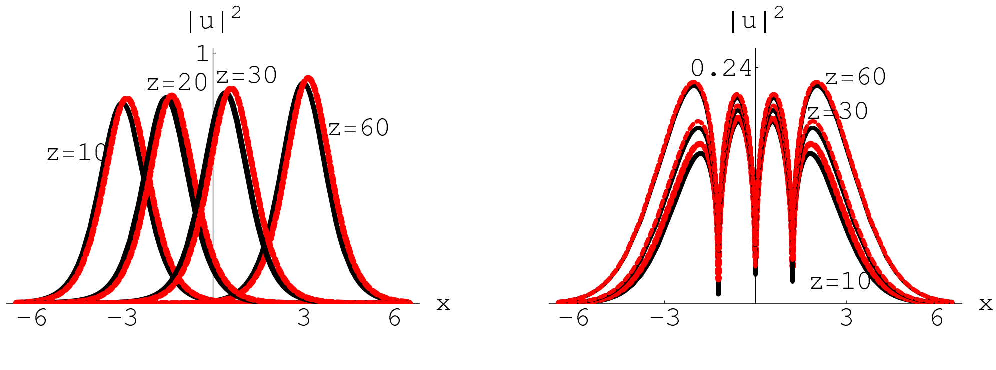

(a) (b)

Figure 5 AF10902E 16SEP2011